The fingerprints of intra-continental deformation in central Europe as envisaged by the synergic use of predicting modelling and geodetic data

A.M. Marotta

Sezione Geofisica, Dipartimento di Scienze della Terra, Università di Milano, Italy

(Received June 21, 2004; accepted September 20, 2004)

ABSTRACT The large scale crustal deformation geodetically observed in Europe is the result of a complex interplay of different geodynamic forces, such as the Africa-Eurasia plates' convergence, the mid-Atlantic spreading and the post-glacial rebound. Each force has a different impact on the deformation in Europe, with tectonic forces playing the major role in the southernmost part of continental Europe, between the Alpine front and the southern border of Fennoscandia, while the post-glacial rebound mainly affects the deformation at high latitudes, north of Potsdam. The lateral rheological heterogeneities also have a crucial role in stiffening the propagation of tectonic deformation throughout northern Europe. When Global Positioning System data are used to constrain predictive geophysical modelling, they reveal their crucial role in distinguishing different geodynamic processes responsible for the observed deformation. A comparison between predicted tectonic deformation and geodetic data demonstrates, in fact, that tectonic forces and post-glacial rebound must be simultaneously taken into account for a correct interpretation of the deformation in northern and central Europe measured by geodetic techniques.

1. Introduction

In the last few years, many international projects have brought major advancements in space geodesy, in terms of improvements of the Global Positioning System (GPS) techniques and in terms of the availability of longer and more reliable GPS position time series. GPS data, acquired in dense networks, sampling different spatial scales, showed their significant potential for monitoring crustal deformation and rate of deformation in various regions, thus allowing one to gain a deep insight into local strain and stress accumulation. Furthermore, when GPS data are used to constrain predictive geophysical modelling, they reveal their crucial role in distinguishing different geodynamic processes responsible for the observed deformation pattern. One of the most suitable laboratories for the fulfilment of this last issue is central Europe, the domain under investigation in the present analysis. Due to the peculiar geographic location of Europe, in fact, the lithospheric deformation is controlled by several geophysical mechanisms, such as the North Atlantic spreading, the continental collision between Africa and Eurasia, the subduction in the Aegean and the Tyrrhenian Seas and the isostatic adjustment after the Pleistocenic deglaciation, all acting on regional scale, or, on a smaller scale, along the sedimentary basins or mountain chains. Although these mechanisms seem to have distinct typologies and range over very different temporal and spatial scales (millions of years and regional scale for the first mechanism and thousands of years and global scale for the second one), they are both still active in Europe and

deform the crust-lithosphere system, inducing velocity and strain rate fields detectable by geodetic techniques (Johansson *et al*., 2002). They must thus be taken into account simultaneously for a correct interpretation of the geodetically retrieved deformation. This work is expected to contribute to understanding the kinematics and dynamics of the crustal deformation processes, and how stress is accumulated and released in central Europe, from Scandinavia to the southern boundary of the Eurasian plate, by means of a combined, analytical and numerical, investigation of tectonic mechanisms and Pleistocenic glacial isostatic adjustment (GIA). The modelling results are compared with deformation measurements contained in the ITRF2000 velocity solutions for central and northern Europe (Altamini *et al*., 2002). As far as the global scale of the GIA process is concerned, I refer to a geophysical methodology (Vermeersen and Sabadini, 1997) that allows us to retrieve the rheological parameters of the lithosphere and mantle by means of a series of global models of the Earth that simulate the response of the planet to global geodynamical processes. The rheological parameters provided by the global Earth models are used as inputs in the numerical models of the Mediterranean, central and northern Europe. The capability of this combined approach has already been demonstrated in a series of previous works (Marotta and Sabadini, 2002, 2004; Marotta *et al*., 2004). This combined modelling approach is necessary for a correct interpretation of the deformation as measured by geodetic techniques. Both the numerical and the analytical model will take into account the physical properties of the crust-lithosphere system and the active tectonic mechanism for Europe and surrounding regions in a self-consistent way. The contributions of GIA and active tectonics will be compared with the geodetic strain based on ITRF2000 velocity solutions. The region under study extends from the Baltic Shield to the southern border of the Eurasiatic plate, along the Magrebid building, the Apennines, the Alps, the Dinarides and the Aegean area.

2. Strain rate in Europe

In order to compare the results of our geophysical modelling with geodetic data, two different representations of the deformation are used, that is the deformation rates calculated along the distance connecting different pairs of geodetic sites, and now on referred as baseline rate (1-D analysis), and the horizontal eigenvectors $\dot{\varepsilon}_1$ and $\dot{\varepsilon}_2$ of the deformation rate tensor, calculated inside triangular areas delimited by three geodetic sites or by three nodes of the numerical grid used for the geophysical modeling (2-D analysis). The comparison between the geodetic and the modeled eigenvalues and eigenvectors allows us to estimate the quality of the geophysical model, in particular its ability to reproduce observations and to predict the evolution of geodynamic processes responsible for the observed deformation pattern.

2.1. 1-D deformation

The baseline rate is formally given by

$$\frac{\partial(BL)}{\partial t} = \left(\vec{V}_1 - \vec{V}_2\right) \cdot \frac{\left(\vec{r}_1 - \vec{r}_2\right)}{\left|\vec{r}_1 - \vec{r}_2\right|}$$

and defines the projection of the relative velocity between two geodetic stations along the direction of the baseline (*BL*) extending from station 1 to station 2. In this way, it is possible to

highlight the 1-D deformation on both short and long wavelengths, according to the distance between the two assumed sites.

The analysis of the 1-D deformation (Fig. 1) indicates that compression characterizes the most of the baseline connecting twin sites along the SW-NE direction (Figs. 1a, 1b, 1c, and 1d), while the extension develops along the baselines directed in the SE-NW direction. In all the panels of Fig. 1, the complex tectonic setting of the Rhine Graben region is evident through the random distribution of compression and extension along the baselines connecting sites distributed in all central Europe with all the sites delimiting the Rhine Graben region.

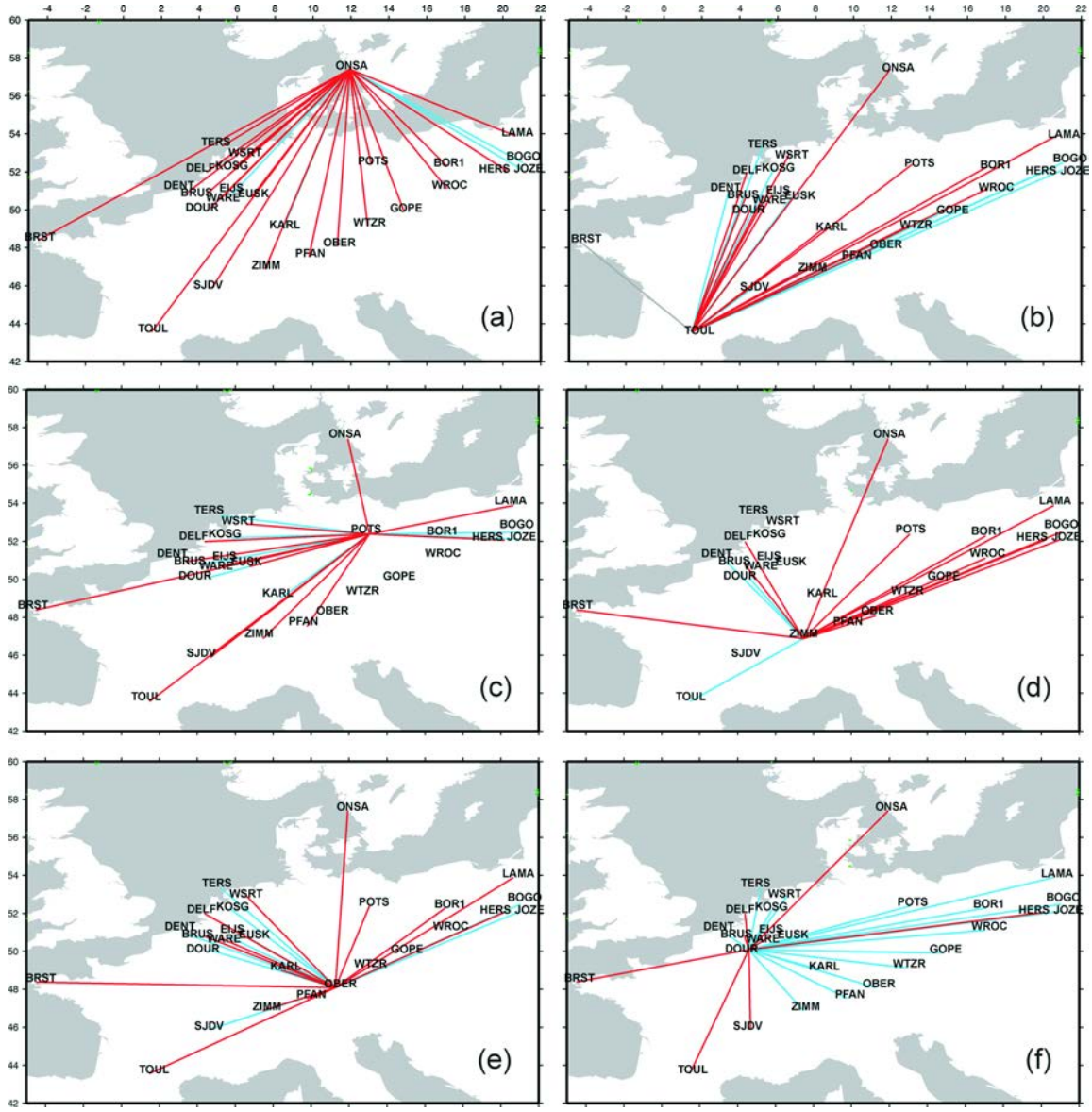

Fig. 1 - Baseline rate derived from ITRF2000 solutions in central Europe. Blue indicates extension and red compression.

2.2. 2-D deformation

The main features highlighted by the 1-D analysis are further confirmed by the analysis of the strain rate eigenvectors' distribution. In order to evaluate the deformation rate tensor, within a set of triangular domains, the strain rate eigenvalues $\dot{\varepsilon}_1$ and $\dot{\varepsilon}_2$ with the azimuth for the second component are computed following the procedure described in Devoti *et al*. (2002). According to this procedure, the strain rate eigenvalues $\dot{\varepsilon}_1$ and $\dot{\varepsilon}_2$ with the azimuth for the component $\dot{\varepsilon}_2$ are computed directly from the horizontal velocity components observed at the vertices of the triangular areas delimited by GPS stations, assuming a linear variation of the horizontal velocity components with respect to their distance. The symmetric component of the velocity gradient tensor yields the eigenvalues and associated eigenvectors of the strain rates. The errors associated to the strain rates are properly propagated from the original covariance matrix of the velocities. The criteria employed to create the triangulation used in the present study is similar to that used by Marotta and Sabadini (2004): a subset of sites where the velocity is known with the lowest variance, is isolated; then the triangulation is chosen to represent homogeneous tectonic units. In the present analysis, two other aspects have been considered in order to improve the reliability of our conclusions. First, only permanent GPS stations have been considered, which should guarantee stable velocity solutions, at least as concerns the last 10 years of GPS observations used to define the ITRF2000 velocity solution database (Altamini *et al*., 2002). Second, the greatest care is devoted to avoiding the fact that any elements of the triangulation should extend through different, major tectonic units; thus, with respect to Marotta and Sabadini (2004), triangles ONSA-POTS-VIS0 and POTS-BOGO-VIS0 are replaced by triangles ONSA-POTS-BOR1, ONSA-BOR1-LAMA and ONSA-LAMA-VIS0 (Fig. 2), placed completely south and north with respect to the Sorgenfrei/Teisseryi-Tornquist Zone; a major faults system playing a crucial role in the deformation decoupling in central Europe (Marotta *et al*., 2001, 2002). For similar reasons, the triangulation in central Europe is almost redefined. The southern limit of the triangulation is now defined by the geodetic sites: TOUL, SJDV, ZIMM, PFAN, WTZR, GOPE and BOR1, all completely north of the Alpine front, to avoid the complex shortening of the Alpine area. An attempt is also made to separate the long wavelength deformation related to the Alpine tectonics in central Europe from the short wavelength deformation in the Rhine Grabens region, delimited by sites DENT, DOUR, 7203, WSRT and KOSG, and more reasonably related to local tectonic processes (es. Bonjer, 1997; Hinzen, 2003). Finally, in order to make the deformation analysis more detailed, more GPS stations have been considered in northern Europe.

Other more sophisticated approaches exist in literature for 2-D strain rate calculations (i.e. Caporali, 2003; Caporali *et al*., 2003), based on the least-square collocation method which enables scattered data and their variances to the nodes of a regular grid to be interpolated. The eigenvectors of the 2-D strain rate eigenvectors are thus computed from the velocity gradient tensor at each interpolation node. Due to the limited number of GPS permanent stations chosen for the present analysis, a statistical analysis would not be significant for the study area, while Devoti *et al*. (2002)'s simpler approach is adopted, which allows a first order approximation of the existing local strain rate pattern.

Table 1 lists the values of strain rate eigenvalues and of the azimuths, with the corresponding errors, computed from ITRF2000 velocity solutions for the final set of triangles.

Fig. 2 shows the corresponding horizontal deformation field in the study domain. Strain rate

eigenvectors $\dot{\varepsilon}_1$ and $\dot{\varepsilon}_2$ indicate a SW-NE directed compression (red bars), while the extension (blue bars) develops in the SE-NW direction. Note that at high latitudes extension always dominates over compression, while at middle latitudes SW-NE directed compression is somewhere comparable to the SE-NW directed extension (triangles WSRT-POTS-ONSA, ONSA-POTS-BOR1, ONSA-BOR1-LAMA and 7303-WSRT-POTS). Another feature that is worth highlighting is the uniform pattern in the direction of compression and extension in central Europe, which fails in the set of triangles BRST-DOUR-DENT, DENT-DOUR-KOSG and KOSG-7203-WSRT. This evidence supports the hypothesis that in the Rhine Graben region the deformation is dominated by local effects (Nocquet *et al*., 2001; Nocquet and Calais, 2003). We

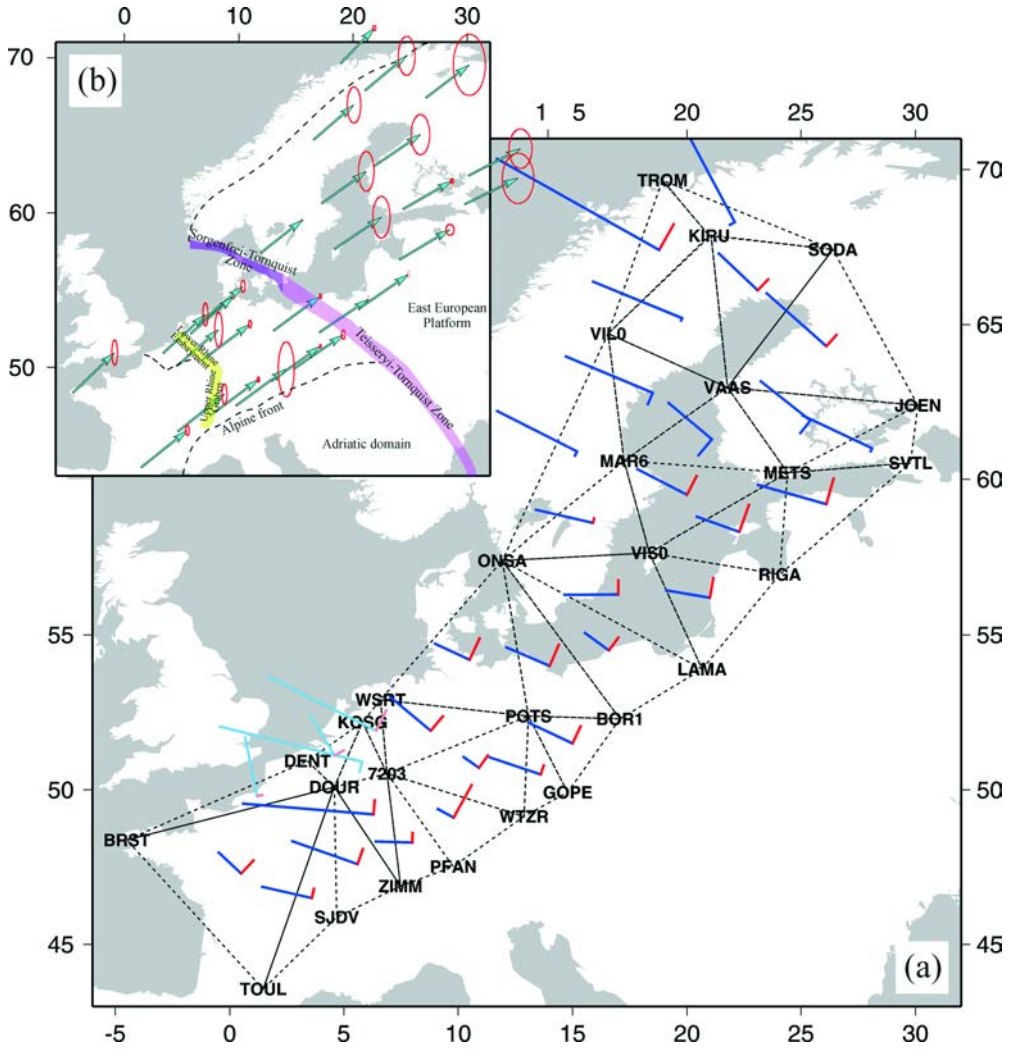

Fig. 2 - (a) Triangular horizontal strain-rate eigenvectors derived from ITRF2000 solutions in central Europe (blue indicates extension and red compression). The light blue and light red colors indicate non-significant strain rates. (b) ITRF2000 velocity vectors (cyan arrows) with 95% confidence region ellipses (red circles) over a simplified sketch of the major tectonic units used to define the triangular mesh for strain-rate computation.

Table 1 - Observed strain rates as deduced from ITRF2000 GPS data.

TRIANGLE	Eigenvalue $\dot{\varepsilon}_1$ nanostrain/yr	Eigenvalue $\dot{\varepsilon}_2$ nanostrain/yr	Azimuth of $\dot{\varepsilon}_2$ degree
TROM-VIL0-KIRU	+19.30±4.80	-3.10±6.90	29.40±7.20
TROM-KIRU-SODA	+10.90±4.00	0.60±17.40	62.00±64.60
POTS-GOPE-BOR1	+5.10±1.40	-2.00±2.90	25.30±12.00
ONSA-BOR1-LAMA	+3.10±0.60	-1.70 ±2.20	36.10±10.10
ONSA-POTS-BOR1	+ 4.90±1.20	-2.40 ±1.60	23.20±6.50
BRST-TOUL-DOUR	+3.20 ±2.50	-1.90±3.70	43.30±19.50
VAAS-SODA-KIR0	+ 5.60±16.60	-1.60±14.60	43.60±63.30
VAAS-KIR0-VIL0	+10.00 ±8.60	0.30±9.30	22.30±42.50
VAAS-METS-JOEN	+6.60 ±8.30	1.70±7.20	38.40±66.90
ONSA-LAMA-VIS0	+5.60 ±3.50	-1.50±11.60	-0.40±39.80
VIS0-LAMA-RIGA	+4.60 ±4.80	-2.10 ±4.40	9.70±46.20
WSRT-POTS-ONSA	+4.00 ±1.20	-2.50±1.30	25.00±7.90
POTS-WTZR-GOPE	+5.60 ±2.90	-1.00 ±2.10	18.50±22.80
ONSA-MAR6-VIL0	+9.30±11.40	0.50 ±3.30	26.90±58.10
ONSA-VIS0-MAR6	+6.10±5.50	-0.50±11.20	13.00±61.10
VIL0-MAR6-VAAS	+9.80±8.60	1.30±10.80	22.70±49.30
VIS0-METS-MAR6	+5.80±6.70	-2.20 ±10.20	27.30±52.50
MAR6-METS-VAAS	+5.90±5.80	2.20±11.00	40.00±95.40
SODA-VAAS-JOEN	+8.30±8.10	-1.60±9.50	41.60±35.00
VIS0-RIGA-METS	+4.70±5.50	-3.00±3.70	19.70±34.10
METS-RIGA-SVTL	+7.40 ±9.60	-2.80±3.70	15.70±39.80
METS-SVTL-JOEN	+8.00±18.40	0.40±17.40	25.30±117.90
7203-ZIMM-PFAN	+3.80 ±7.50	-1.00±3.70	1.50±154.40
WTZR-7203-PFAN	+1.90 ±1.90	-3.90±16.60	28.90±62.30
7203-WTZR-POTS	+2.00 ±1.00	-1.60±1.20	35.30±12.10
DOUR-ZIMM-7203	+13.60±4.20	-1.50±4.20	4.70±32.60
7203-POTS-WSRT	+5.50±2.80	-2.00±2.20	39.80±17.90
BRST-DOUR-DENT	+6.20±28.20	-0.60±2.00	78.50±32.50
DENT-DOUR-KOSG	+4.80±23.20	-1.10±6.60	59.00±55.00
DOUR-7203-KOSG	+15.20±5.00	1.10±10.10	13.90±25.40
KOSG-7203-WSRT	+12.50±6.10	-2.40±9.30	26.70±15.00
TOUL-SJDV-DOUR	+5.30±4.30	-1.00±4.70	12.70±63.00
SJDV-ZIMM-DOUR	+7.20±2.90	-1.70±6.90	19.40±23.40

must note that the GPS velocities at the corners of each triangle have different uncertainties (Fig. 2b), some of which relatively high (e.c. ZIMM, DOUR and, in general, all the station at high latitudes). This has a significant impact on the strain rate uncertainty computation, as Table 1 shows.

3. Geophysical modelling

In the next two sections (3.1. and 3.2.) the observed deformation is compared with that predicted by the two kinds of geophysical models, related to tectonics and GIA. In this regard, we must note that the GPS velocities used in this paper are derived from relatively short observation time spans (around 10 years) with respect to the time scale of the geological processes taken into

consideration. As a consequence, only the assumption of considering tectonic loading as a steady-state process allows us to compare modelling results and observations.

3.1. Tectonics

The first class of models analyzes the effects of the tectonic forces, that acted in the past and that are eventually still active in the region under study, on the deformation in central and northern Europe. A numerical approach is used to study the variation in time of the regional deformation field for a given geometry and active tectonic forces. The employment of finite element techniques allows a great flexibility of the modelling, in particular, with respect to the use of complex geometries and horizontal rheological heterogeneities. The spherical numerical approach developed in Marotta *et al*. (2004) is used. The reader is requested to deal with that paper for a full description of the modelling approach; herein, only the major elements of the numerical model are mentioned. By taking as starting point an incompressible viscous lithospheric system of uniform thickness and rheology, in isostatic equilibrium over a half infinite space of inviscid asthenosphere, lateral heterogeneities in the rheological properties and in the thickness are implemented within a thin-sheet approximation, which assumes that the lithospheric thickness is small compared to the wavelength of the applied loads. In fact, Europe is characterized by several basin systems (e.g. Danish Basins, German Basins, Pannonic Basins and Polish Basins) and by the wide Baltic Shield in the northern part of the studied region, which cause significant lateral contrasts in the local strength and crust and lithosphere thickness. The long time-scale tectonic deformation in central Europe is analyzed by solving the momentum equations in spherical coordinates and a steady-state:

$$\frac{1}{r}\frac{\partial \sigma_{\theta\theta}}{\partial \theta}+\frac{1}{r\sin\theta}\frac{\partial \sigma_{\theta\phi}}{\partial \phi}+\frac{\partial \sigma_{\theta r}}{\partial r}+\frac{1}{r}\left[\left(\sigma_{\theta\theta}-\sigma_{\phi\phi}\right)\cot\theta+3\sigma_{\theta r}\right]=0$$

$$\frac{1}{r}\frac{\partial \sigma_{\phi\theta}}{\partial \theta}+\frac{1}{r\sin\theta}\frac{\partial \sigma_{\phi\phi}}{\partial \phi}+\frac{\partial \sigma_{\phi r}}{\partial r}+\frac{1}{r}\left[3\sigma_{\phi r}+2\sigma_{\phi\theta}\cot\theta\right]=0$$

$$\frac{1}{r}\frac{\partial \sigma_{r\theta}}{\partial \theta}+\frac{1}{r\sin\theta}\frac{\partial \sigma_{r\phi}}{\partial \phi}+\frac{\partial \sigma_{rr}}{\partial r}+\frac{1}{r}\left[2\sigma_{rr}-\sigma_{\theta\theta}-\sigma_{\phi\phi}+\sigma_{r\theta}\cot\theta\right]+f_r=0$$

where θ, ϕ and r represent the co-latitude (south), east-longitude and radial distance from the Earth's center and f_r denotes the gravitational body force term. As usual, the stress can be expressed as $\sigma_{ij}=\tau_{ij}-p_o\sigma_{ij}$, where τ_{ij} is the deviatoric stress and p_o is the hydrostatic pressure. For a Newtonian viscous medium, the deviatoric viscous stress is related to the strain rate $\dot{\varepsilon}_{ij}$ by $\tau_{ij}=2\mu\dot{\varepsilon}_{ij}$. Under the assumption that only horizontal tectonic forces are active and that basal shear stresses are absent, the thin sheet approximation allows to reduce the three momentum equations into two equations, after integration over the thickness of the lithosphere [see Appendix A in Marotta *et al*. (2004) for the detailed procedure]:

$$\frac{\partial}{\partial \grave{e}}\left[2\overline{\mu}\left(\frac{\partial}{\partial\theta}u_\theta + u_r\right)\right] + \frac{1}{\sin\theta}\frac{\partial}{\partial\phi}\left[\overline{\mu}\left(\frac{1}{\sin\theta}\frac{\partial}{\partial\phi}u_\theta + \frac{\partial}{\partial\theta}u_\phi - u_\phi\cot\theta\right)\right] +$$
$$\left[2\overline{\mu}\left(\frac{\partial}{\partial\theta}u_\theta - \frac{1}{\sin\theta}\frac{\partial}{\partial\phi}u_\phi - u_\phi\cot\theta\right)\right]\cot\theta = \frac{g\rho_c R}{2L}\left(1-\frac{\rho_c}{\rho_m}\right)\frac{\partial}{\partial\theta}S^2$$

$$\frac{\partial}{\partial \grave{e}}\left[\overline{\mu}\left(\frac{1}{\sin\theta}\frac{\partial}{\partial\phi}u_\theta + \frac{\partial}{\partial\theta}u_\phi - u_\phi\cot\theta\right)\right] + \frac{1}{\sin\theta}\frac{\partial}{\partial\phi}\left[2\overline{\mu}\left(\frac{1}{\sin\theta}\frac{\partial}{\partial\phi}u_\theta + u_\theta\cot\theta + u_r\right)\right] +$$
$$\left[2\overline{\mu}\left(\frac{\partial}{\partial\phi}u_\theta + \frac{1}{\sin\theta}\frac{\partial}{\partial\phi}u_\theta + -u_\phi\cot\theta\right)\right]\cot\theta = \frac{g\rho_c R}{2L}\left(1-\frac{\rho_c}{\rho_m}\right)\frac{1}{\sin\theta}\frac{\partial}{\partial\phi}S^2$$

where $\overline{\mu}$ denotes the vertically averaged viscosity of the lithosphere, S is the crustal thickness, L the lithosphere thickness, ρ_c (2800 kg/m^3) and ρ_m (3200 kg/m^3) are the density of the crust and of the mantle, respectively, g is the gravity (9.81 m/s^2) and R the radius of the Earth.

The study domain ranges from the mid-Atlantic ridge and from the Africa-Eurasia plate contact to the 45° E meridian (Fig. 3) and is discretized by small planar finite triangular elements of varying size (1°±1° in central Europe; Fig. 3). Under the peculiar assumptions of the used thin sheet numerical approach (Marotta *et al*., 2004), once the crustal and lithospheric thickness, the density of crust and lithosphere are assigned, the horizontal components of velocity field can be predicted. Eleven tectonic model types have been performed, different for horizontal rheological heterogeneities and boundary conditions. They are listed as models 1÷8 and 18÷20 in Table 2. The lateral variations in lithospheric strength are implemented by assigning a different stiffness to each element of the model grid. In this regard, an average viscosity of 10^{25} Pa·s is assigned to the reference European domain; this particular choice guarantees numerical stability once lateral viscosity variations are introduced into the model, as already demonstrated in Marotta *et al*. (2004). Two other lithospheric domains are considered in the analysis (Fig. 3). The Mediterranean domain, extending through the Adriatic Plate, now on called Adria, and the East European Platform from now on called Baltic. An average viscosity of one order of magnitude less than the reference European domain is assigned to Adria (soft Mediterranean domain). This assumption should account for the complexity of this region, that is an assemblage of different structural units (e.g., the Adriatic plate, Tyrrhenian Sea, and Pannonian Basin), at least for the long wavelength deformation. The second lithospheric domain, Baltic, is assumed two orders of magnitude stiffer than the reference European domain [stiff Baltic domain; Marotta *et al*. (2001, 2002)].

The boundary conditions are the same used in Marotta *et al*. (2004). They are parametrized in terms of velocities, being, for the thin sheet assumption, constant through the lithosphere thickness. An Africa-Eurasia continental convergence of the order of 1 cm/yr is prescribed according to NUVEL-1A (green arrows) (DeMets *et al*., 1994). The line-ridge push forces are parameterized in terms of velocity boundary conditions applied along the ridge and ranging from 0.0 to maximuum 10.0 mm/yr (equivalent to a symmetric spreading rate deduced from NUVEL-1A) (yellow arrows). Along the Aegean trench the velocity boundary conditions are obtained

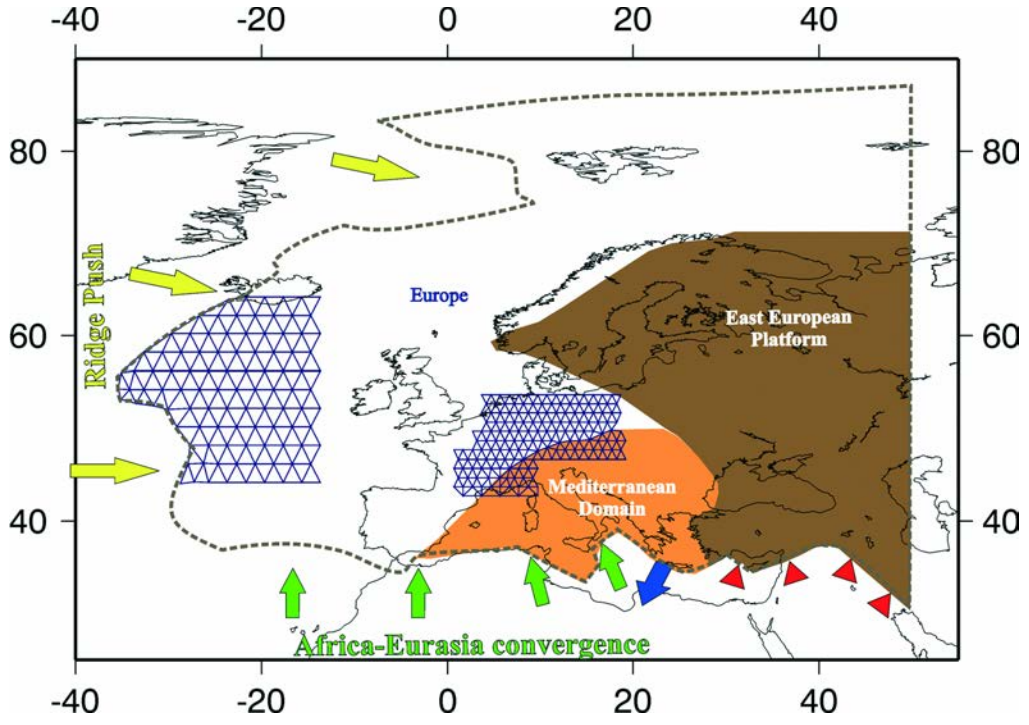

Fig. 3 - Geometry of the domain under study (dashed line) and boundary conditions used in the numerical analysis. See text for details.

from McClusky *et al*. (2000) and reflect the horizontal component of the trench subduction forces (blue arrow). Along the eastern boundary the east component of the velocity and the shear stress are fixed to zero. In the south-eastern part of the study domain the deformation is controlled by the shear motion along the North Anatolian Fault (Mantovani *et al*., 2001; Jiménez-Munt and Sabadini, 2002). In particular, Jimenez-Munt and Sabadini (2002) show that the North Anatolian Faults system is responsible for little long-wavelength deformation at medium and high latitudes, where the ITRF2000 sites considered in this analysis are located. For this reason, the border between the East European Platform and Arabian Plate is kept fixed (red triangles).

3.1.1. Tectonic deformation

In this section, we analyse the effects of rheological heterogeneities and boundary conditions on the predicted deformation field, in terms of velocity and strain rate fields. With respect to the list of Table 2, only the tectonic models which showed the most significant results will be discussed.

No rheological heterogeneities

Fig. 4 portrays the velocity field predicted by tectonic models 1 (Fig. 4a) and 3 (Fig. 4b). These models neglect lateral rheological heterogeneities and allow us to highlight the effects of the Atlantic Ridge push, when the intensity of this line force is progressively reduced to zero, to simulate the complete retainment of ridge push force within the oceanic Atlantic lithosphere. This

Table 2 - List of tectonic models considered in the analysis. Notation: Homo = no rheological heterogeneities; Baltic = stiff East European Platform; Adria = soft Mediterranean domain; V. S., 1997 = Vermeersen and Sabadini (1997).

Model	Characteristic	Ridge velocity boundary conditions (mm/yr)
1	Homo	0.0
2	Homo	1.0
3	Homo	5.0
4	Homo	10.0
5	Baltic	0.0
6	Baltic	5.0
7	Adria	0.0
8	Adria	5.0
9 a/b	GIA21/22	V.S., 1997
10 a/b	Homo + GIA21/22	0.0
11 a/b	Homo + GIA21/22	1.0
12 a/b	Homo + GIA21/22	5.0
13 a/b	Homo + GIA21/22	10.0
14 a/b	Baltic + GIA21/22	0.0
15 a/b	Baltic + GIA21/22	5.0
16 a/b	Adria +GIA21/22	0.0
17 a/b	Adria + GIA21/22	5.0
18	Baltic + Adria	0.0
19	Baltic + Adria	5.0
20	Baltic + Adria	10.0
21 a/b	Baltic + Adria + GIA21/22	0.0
22 a/b	Baltic + Adria + GIA21/22	5.0
23 a/b	Baltic + Adria + GIA21/22	10.0

last case is portrayed in Fig. 4a, and shows a straightforward control of deformation by Africa-Eurasia convergence. In fact, the velocity field progressively decreases in intensity from the south to the north, with the iso-contours expanding roughly parallel to the Alpine front and the direction remains NW-directed throughout Europe, up to the highest latitude, north of 70° where the effects of tectonics become negligible. When the intensity of the ridge push force is increased, the predicted velocity field shows a progressive rotation from NW to NE of the direction of velocities in central and northern Europe (Fig. 4b), with a significant increase of the intensity of velocities in the western part of the study domain.

In order to analyse the area deformation due to tectonic forces for the same models discussed above, for each triangular element of the numerical grid the principal horizontal strain rate eigenvectors $\dot{\varepsilon}_1$ and $\dot{\varepsilon}_2$ are computed following the procedure specified in paragraph 2.1 (Fig. 5). The bars represent the two horizontal eigenvectors, with their magnitude and direction. The color map represents the strain rate regime. Blue indicates extension and red indicates compression both for the bars and for the map.

Fig. 5a shows the predicted maximum horizontal strain rate for model 1, when the ridge push forces are neglected. A broad scale of almost-uniform SE-NW compression is evident in central Europe, which decreases into the Fennoscandia domain. Extension appears only in the

easternmost portion of the East European Platform. These features are in contrast with the data (compare Fig. 5 with Figs. 1 and 2). Geophysical predictions get worse when the intensity of the ridge push force is increased (Fig. 5b); two main changes clearly appear in the strain rate field in central and northern Europe: first, a significant increase of compression in Fennoscandia where extension is not present; secondly, a further SE-NW rotation of the direction of compression, totally in contrast with the GPS data.

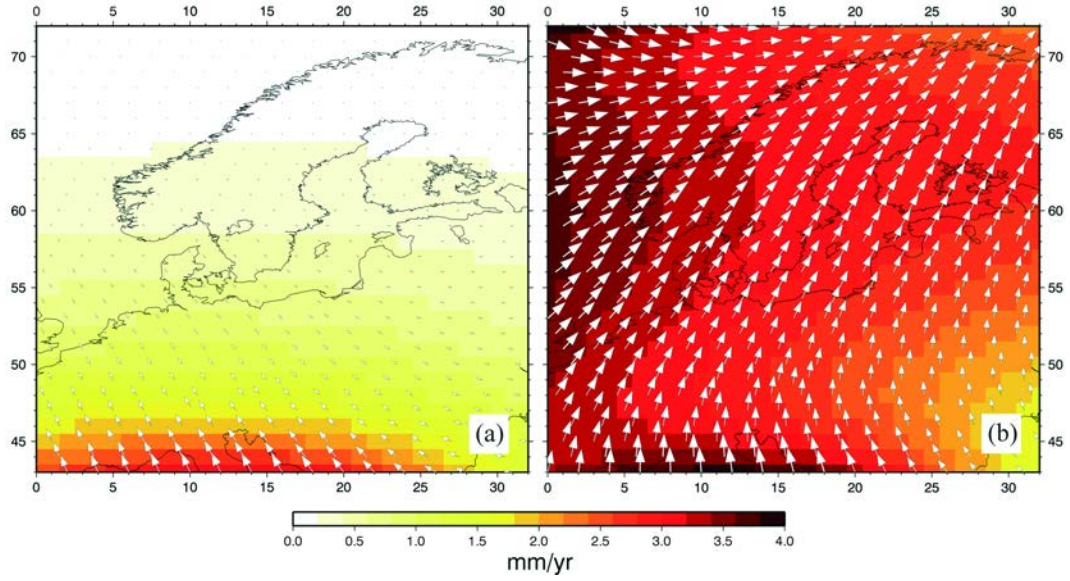

Fig. 4 - Horizontal velocity field predicted by the tectonic models 1 (a) and 3 (b).

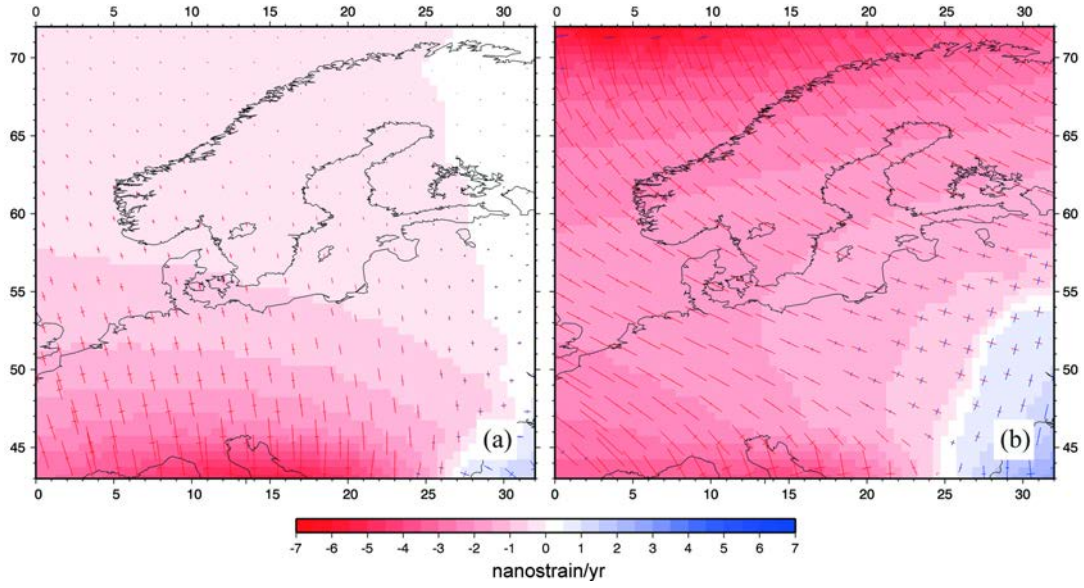

Fig. 5 – Maximum horizontal strain rate predicted by the tectonic models 1 (a) and 3 (b). Blue indicates extension and red compression.

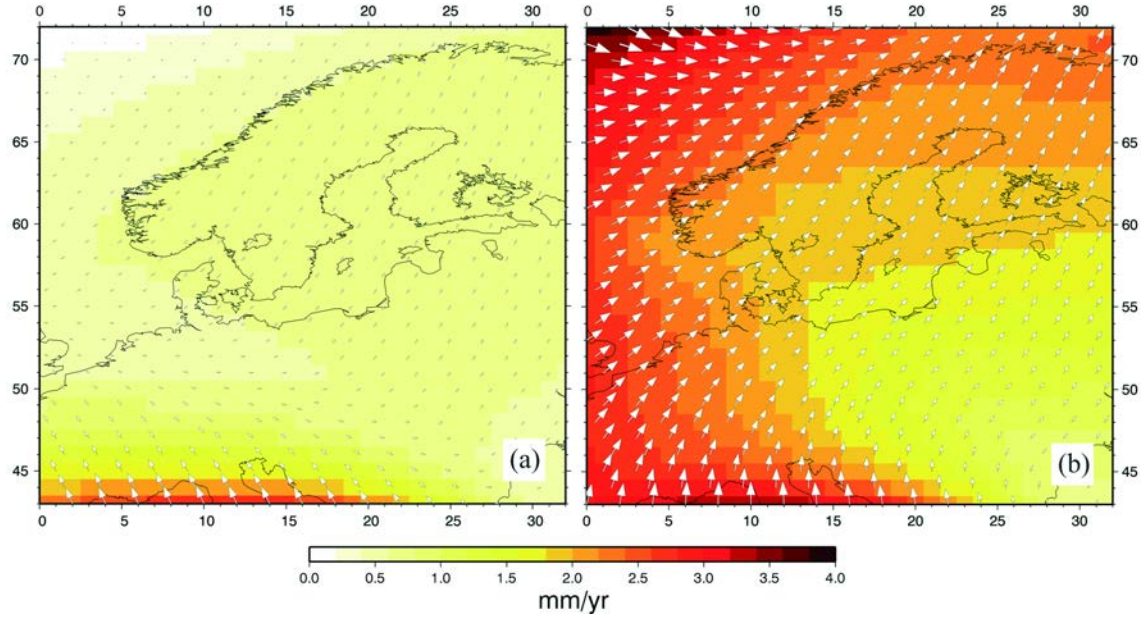

Fig. 6 - Horizontal velocity field predicted by the tectonic models 5 (a) and 6 (b).

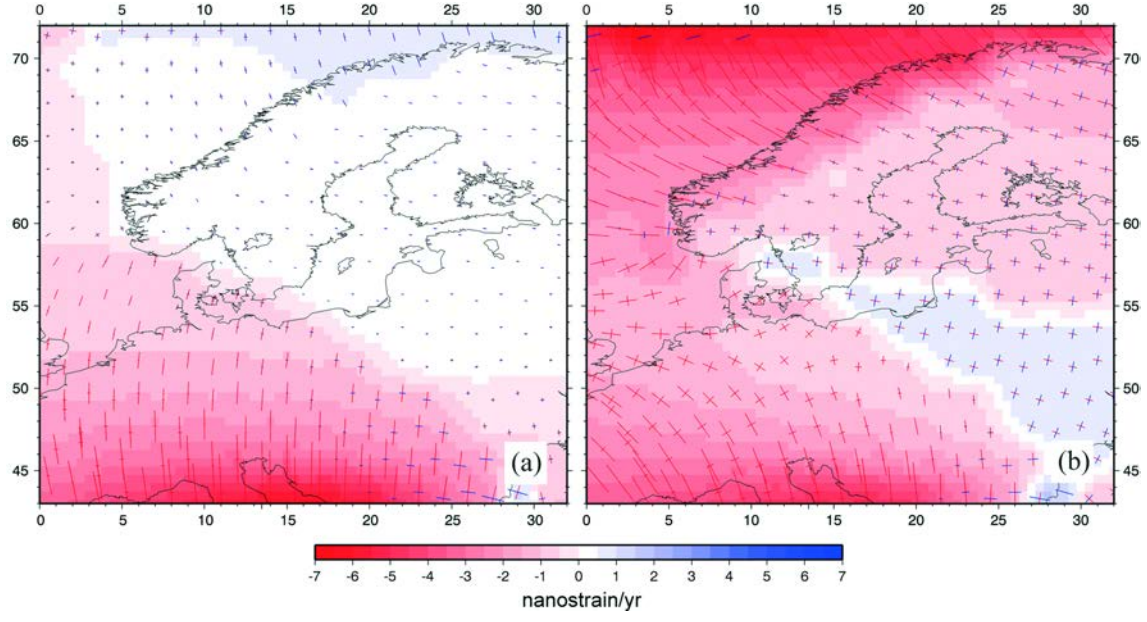

Fig. 7 - Maximum horizontal strain rate predicted by the tectonic models 5 (a) and 6 (b). Blue indicates extension and red compression.

Stiff Baltic domain

As already shown in Marotta and Sabadini (2002) for a smaller region and a flat Earth, the incorporation of lateral rheological heterogeneities in the lithosphere has a crucial role in the predicted velocity and deformation patterns in northern Europe. The next two figures show the effects of assuming a stiff Baltic domain in the spherical model that is used in the present study (in terms of a viscosity value two orders of magnitude higher than in the rest of the study domain).

Figs. 6 and 7 indicate that the effects of a stiff Baltic domain are different for high and low intensity of the ridge push force. In the first case, a stiff Baltic domain acts as a barrier for the propagation of deformation at the high latitudes, significantly reducing the intensity of the velocity field in the Fennoscandian area, where strong gradients grow, with velocity ranging from 2 to 3 mm/yr (Fig. 6b), while a nearly constant velocity of 3 mm/yr is predicted by the homogeneous model with the same boundary conditions (Fig. 4b). If the ridge push force is set to zero, the longitudinal push effects disappear and a peculiar SW directed velocity field is driven at high latitudes by the lateral rheological heterogeneities (Fig. 6a). This new velocity field is responsible for significant changes in the deformation field. First, extension is induced through the Fennoscandian domain. Secondly, a clockwise rotation occurs in the maximum horizontal compressive eigenvectors in central Europe, with a new local strain pattern more in agreement with the observations (Fig. 7a). The results showed in Fig. 7b support the hypothesis of ridge push forces totally absorbed by the Atlantic oceanic lithosphere before reaching central Europe.

Soft Mediterranean domain

Model 18 is defined as model 5 but with a one order of magnitude reduction of the viscosity within the Mediterranean lithosphere. Refering to a model carrying solely the stiffened East European Platform, lowering the viscosity in the Mediterranean domain has two main effects: modifying the predicted direction of motion in Fennoscandia from NE-SW to SW-NE and reducing the magnitude of the velocity from 0.8-1.0 mm/yr to 0.2-0.3 mm/yr in the same region (Fig. 8).

Fig. 9 shows the maximum strain rate eigenvectors corresponding to the velocity field portrayed in Fig. 8. A comparison between Fig. 9 and Fig. 7a indicates that the largest amount of deformation driven by the boundary conditions concentrates in the weakened lithosphere of the Mediterranean, with a sensitive impact into the intra-plate deformation in central and northern Europe, where the deformation rate becomes negligible.

3.1.2. Predicted versus observed deformation

The intra-continental deformation, predicted by our numerical modelling in central and northern Europe, is now compared with the observed deformation, based on IRTF2000 velocity solutions. In order to do this, the strain rate eigenvectors are computed for the same set of triangular domains shown in Fig. 2, on the base of the modelled horizontal components of the velocities; then, the results are compared with the corresponding observed quantities (Fig. 10), already shown in Fig. 2. The results of this comparison are discussed in relation to the previous similar work by Marotta and Sabadini (2004). Although in the present study a different set of triangular domains is used with respect to Marotta and Sabadini (2004), many features are

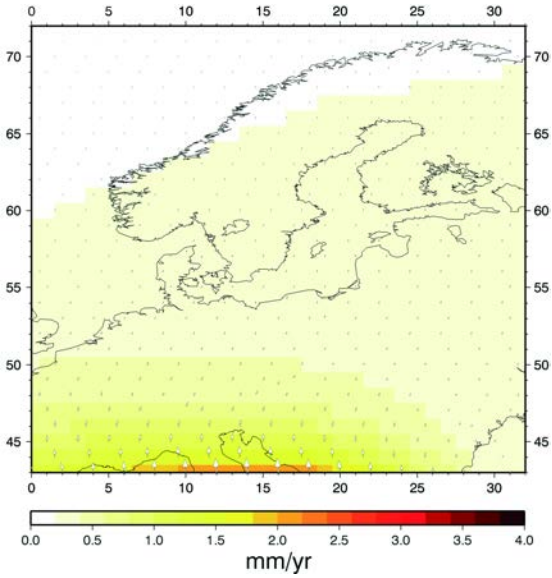

Fig. 8 - Horizontal velocity field predicted by the tectonic model 9.

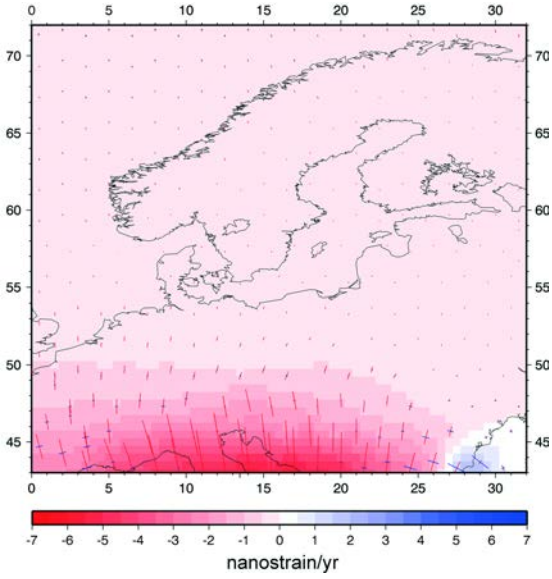

Fig. 9 - Maximum horizontal strain rate predicted by the tectonic models 9. Blue indicates extension and red compression.

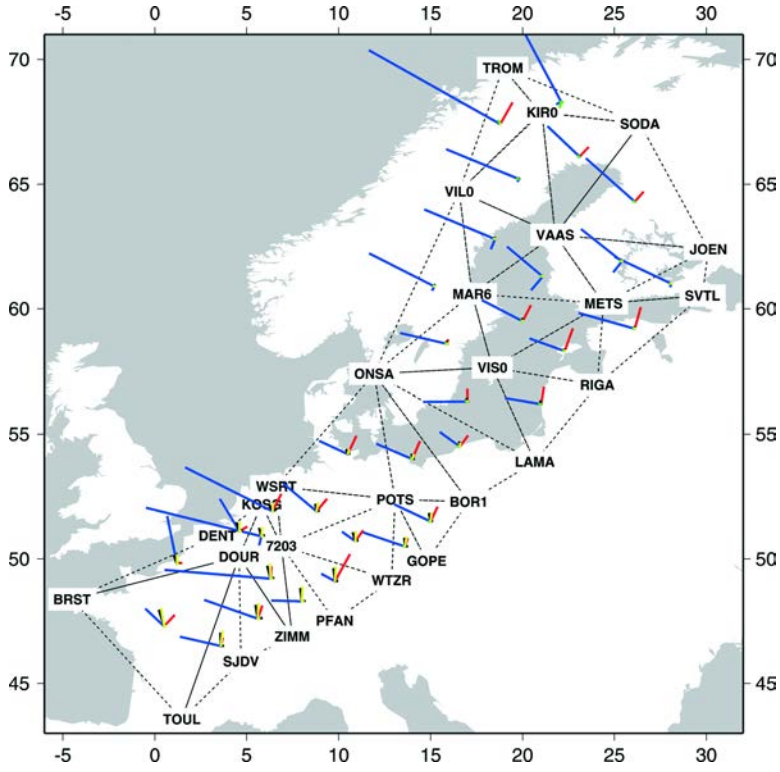

Fig. 10 - Triangular strain-rate eigenvectors predicted by tectonic models 1 (black-compression and cyan-extension bars) and 5 (yellow-compression and green-extension bars), compared with observed strain-rate eigenvector (red-compression and blue-extension bars).

insensitive to that change. This fact strengthens the main conclusions of Marotta and Sabadini's (2004) works; furthermore, it induces one to discuss herein only the different aspects predicted by the geophysical modelling.

The analysis of Fig. 10 confirms the conclusions of the area deformation analysis. That is, while the predicted eigenvalues of strain rate is mainly controlled by the velocity boundary conditions (the Africa-Eurasia convergence in the study case represented in Fig. 10), the azimuths of the eigenvectors strain rate are constrained by the rheological lateral heterogeneities. The tectonic model accounting for a stiff Baltic domain fits the GPS data better, at least in central Europe, while the propagation of tectonic flow in the Fennoscandia area is negligiable. Finally, the results shown in Fig. 10 support the hypothesis that, in this area the deformation is controlled by local events, not accounted for in our tectonic models, rather than by the regional Alpine tectonics. However, although the discussed improvement occurs at low latitudes, the observed deformation in the Fennoscandia domain remains underestimated by a solely tectonic prediction.

3.2. Glacial isostatic adjustment

A new evaluation of the strain rate eigenvectors is performed for the set of triangles shown in Fig. 2 accounting for the deformation induced by GIA. The GIA models are the same as those by Marotta and Sabadini (2002). Models shown in Fig. 11 are characterized by an upper mantle viscosity of $0.5 \cdot 10^{21}$ Pa·s , up to the base of the lithosphere, and a lower mantle viscosity of 10^{21} Pa·s, GIA21, or 10^{22} Pa·s , GIA22. A 120 km-thick lithosphere of 10^{25} Pa·s is considered, as in the tectonic models.

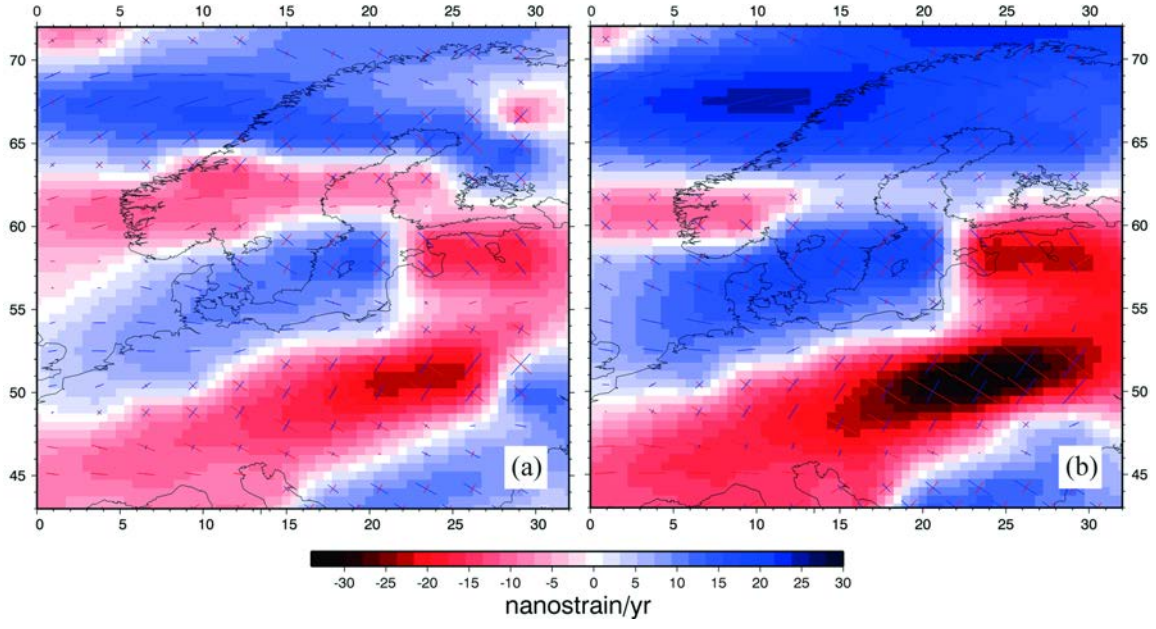

Fig. 11 - Horizontal strain-rate predicted by models GIA21 (a) and GIA22 (b).

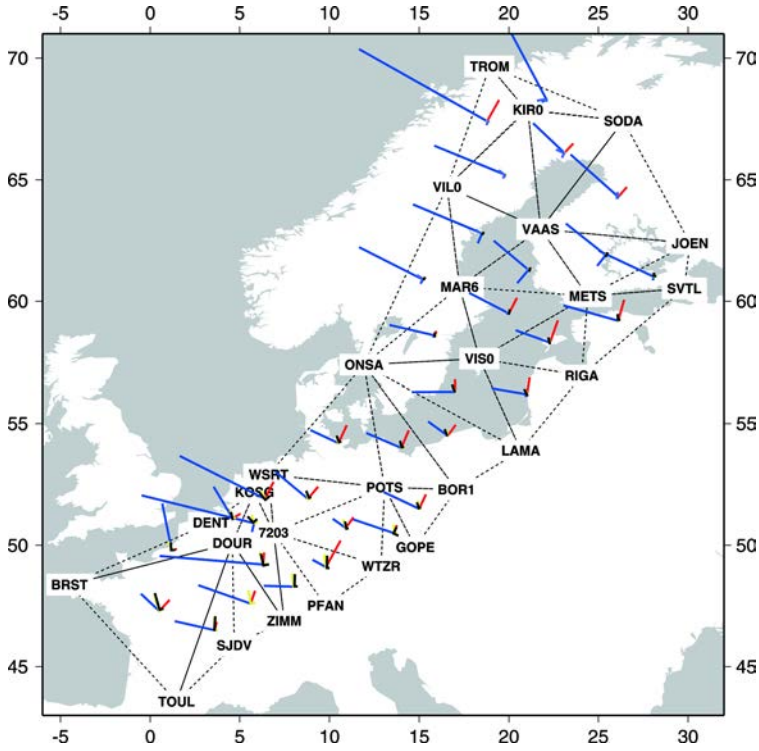

Fig. 12 - Triangular strain-rate eigenvectors predicted by the combined model 14a (black-compression and cyan-extension bars), compared with those predicted by the tectonic models 5 (yellow-compression and green-extension bars) and those deduced by the ITRF2000 velocity solutions (red-compression and blue-extension bars).

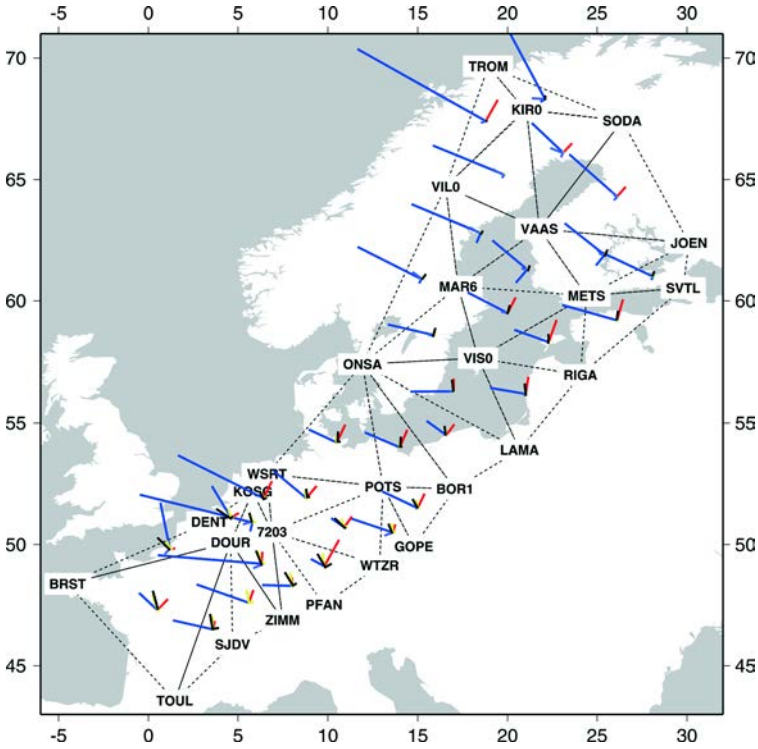

Fig. 13 - Triangular strain-rate eigenvectors predicted by the combined model 14b (black-compression and cyan-extension bars), compared with those predicted by the tectonic models 5 (yellow-compression and green-extension bars) and those deduced by the ITRF2000 velocity solutions (red-compression and blue-extension bars).

Both GIA21 and GIA22 predict SE-NW compression and SW-NE extension at low and high latitudes, while the opposite regime is predicted at intermediate latitudes [see Fig. 2 in Marotta and Sabadini (2002) for details about the velocity fields predicted by models GIA21 and GIA22]. The comparison between the two horizontal eigenvectors allows us to distinguish an alternating sequence of extension and compression throughout central and northern Europe, with compression mainly located in proximity to the Mediterranean, the maximum compression being in the Pannonian region. The maximum extension is predicted in the Fennoscandia area, as the ITRF2000 velocity solutions indicate (compare Fig. 11 and Fig. 2).

Fig. 12 shows the triangular strain rate eigenvectors predicted by the combined model 14a (black-compression and cyan-extension bars), compared with those predicted by the tectonic models 5 (yellow-compression and green-extension bars) and those deduced by the ITRF2000 velocity solutions (red-compression and blue-extension bars). Fig. 13 shows the same for combined model 14b.

In case model GIA21 is considered (Fig. 12) and when the effects of GIA are combined with the effects of tectonics, an improvement of the fit between predictions and observation is achieved, in particular for the azimuth of the compressive component of strain-rate eigenvectors in central Europe. At high latitudes the GIA21 model reproduces, solely, a small fraction of the observed extension. A slighty increase in the extension in the Fennoscandia region is obtained by combining tectonic model 5 with model GIA22 (Fig. 13). However, the improved fit at high latitudes is accompanied by a counter-clockwise rotation of the strain-rate eigenvectors predicted by the combined model 14b, getting a local worsening of the fit.

The comparison between Fig. 12 and Fig. 13 highlights the necessity to consider lateral rheological heterogeneities also within a global model used to predict the GIA-related component of deformation. Another point that must be discussed in relation with the prediction of the GIA models used is that in both cases the predicted deformation is significantly lower with respect to the observed one. According to the previous discussion, this evidence is not related to the absence of lateral rheological heterogeneities in the GIA model used; more precisely, it is related to other reasons, such as the usage of a viscosity profile derived from time-dependent gravity study (Sabadini *et al*., 2002) or to the incompressibility of the global model.

4. Final remarks

The joint use of different advanced geophysical models to predict intra-continental deformation in Europe, taking into account the effects induced both by tectonics and GIA, allows us to highlight the fundamental role of geodetic data in distinguishing among different geodynamic scenarios.

The present analysis indicates that the ridge-push forces is totally absorbed by the Atlantic oceanic lithosphere before reaching central Europe and that the lithospheric deformation in central and northern Europe is the result of two major geodynamic mechanisms, the NW-SE Africa-Eurasia plate convergence and the GIA, both still active; the former plays the major role up to the southern border of the East European Platform, while the latter controls deformation at the highest latitudes.

The comparison between predictions and data differs in several aspects from that of Marotta and Sabadini (2004). First, only permanent GPS stations are considered, to guarantee stable velocity solutions. Second, a new set of triangular areas covering the study domain is now used, taking into account important tectonic features characterizing the study domain (i.e. the Trans European Suture Zone and the Rhine Graben Region), not included in Marotta and Sabadini (2004). The new redefined triangulation allows us to improve the fit between data and predictions in the area between the Alpine Front and the southern border of the Rhine Graben Region, where deformation seems to be controlled by local tectonics. The discrepancies still present between data and prediction at high latitude do not seem to be related to the particular set of triangular areas where the analysis is performed, rather to limitation of the GIA modelling approach, such as the assumed incompressibility of the medium. Work to account for compressibility is ongoing, with the purpose of quantitatively testing this hypothesis.

4.1. Present limitations and future development of the analysis

A limitation of the model is related to the definition of the boundary conditions. The use of NUVEL-1A velocities to define the kinematic boundary conditions along the Africa-Europe southern boundary of the model is a problematic aspect of the model. Some recent papers (i.e. Altamini *et al*., 2002) suggest that NUVEL-1A model is not able to describe the present-day kinematics observed in the Mediterranean area, where the observed velocities seem to be around 50% lower than the ones predicted by the NUVEL-1A model. A sensitivity analysis of the effects of such bias in the modelled strain-rate was quantitatively performed in a previous analysis (Marotta and Sabadini, 2004), in which it was demonstrated that a 50% change in the observed velocity values reflects in a variation of the same order on the computed strain rates. This crucial aspect of the model is currently under study. The usage of observed geodetic velocities to define more suitable boundary conditions is expected to induce a significant reduction of the discrepancy between observed and modelled strain rates.

The model will also benefit from the inclusion of local geological structures like fault and basin systems in the central part of the study area, where the discrepancy between observed and modelled strain rate is higher.

Acknowledgements. This research was funded by the Italian Ministry of Universities and Research (M.I.U.R.) under the project entitled “A multidisciplinary monitoring and multiscale study of the active deformation in the northern sector of the Adria plate” (COFIN 2002). The author thanks Roberto Sabadini for fruitful discussions during the preparation of the manuscript. The author also thanks A. Caporali and an anonymous reviewer for their comments and suggestions. All figures were created using GMT plotting software (Wessel and Smith, 2001). This paper was presented during the 22nd National Conference of the “Gruppo Nazionale di Geofisica della Terra Solida”, held in Rome from November 18 to 20, 2003.

REFERENCES

Altamini Z., Sillard P. and Boucher C.; 2002: *ITRF2000: a new release of the International Terrestrial Reference Frame for Earth Science applications*. J. Geophys. Res., **107**, 2001JB000561.

Bonjer K.P.; 1997: *Seismicity pattern and style of seismic faulting at the eastern borderfault of the southern Rhine Graben*. Tectonophysics, **275**, 41-69.

Caporali A.; 2003: *Average strain rate in the Italian crust inferred from a permanent GPS network – I. Statistical analysis of the time-series of permanent GPS stations*. Geophys. J. Int., **155**, 241-253.

Caporali A., Martin S. and Massinori M.; 2003: *Average strain rate in the Italian crust inferred from a permanent GPS network – II. Strain rate versus seismicity and structural geology*. Geophys. J. Int., **155**, 254-268.

DeMets C., Gordon R.G., Argus D.F. and Stein S.; 1994: *Effect of recent revisions to the geomagnetic reversal timescale on estimates of current plate motions*. Geophys. Res. Lett., **21**, 2191-2194.

Devoti R., Ferraro C., Lanotte R., Luceri V., Nardi A., Pacione R., Rutigliani P., Sciarretta C., Gueguen E., Bianco G. and Vespe F.; 2002: *Geophysical interpretation of geodetic deformations in the central Mediterranean area*. Tectonophysics, **346**, 151-167.

Hinzen K.G.; 2003: *Stress field in the North Rhine area, central Europe, from earthquake fault plane solutions*. Tectonophysics, **377**, 325-256.

Jimenez-Munt I. and Sabadini R.; 2002: *The block-like behaviour of Anatolia envisaged in the modelled and geodetic strain*. Geophys. Res. Lett. **29**, 39/1-39/4.

Johansson J.M., Davis J.L., Scherneck H.-G., Milne G.A., Vermeer M., Mitrovica J.X., Bennett R.A., Jonsson B., Elgered G., Elósegui P., Koivula H., Poutanen M., Rönnäng B.O. and Shapiro I.I.; 2002: *Continuous GPS measurements of postglacial adjustment in Fennoscandia 1. Geodetic results*. J. Geophys. Res., **107**, B8, 2157, doi:10.1029/2001JB000400.

Mantovani E., Celli N., Albarello D., Viti M., Babbucci D., Tamburrelli C. and D'Onza F.; 2001: *Numerical simulation of the observed strain field in the central-eastern Mediterranean region*. J. of Geodyn., **31**, 519-556.

Marotta A.M. and Sabadini R.; 2002: *Tectonic versus glacial deformation in Europe.* Geophys. Res. Lett., **29**, 73/1-73/4.

Marotta A.M. and Sabadini R.; 2004: *The signature of tectonics and glacial isostatic adjustement revealed by the strain rate in Europe*. Geophys. J. Int., **157**, 865-870.

Marotta A.M., Bayer U., Scheck M. and Thybo H.; 2001: *The stress field below the NE German Basin: effects induced by the Alpine collision*. Geophys. J. Int., **144**, F8-F12.

Marotta A.M., Bayer U., Thybo H. and Scheck M.; 2002: Origin of the regional stress in the North German Basin: Results from numerical experiments. Tectonophysics, **360**, 245-264.

Marotta A.M., Mitrovica J.X., Sabadini R. and Milne G.; 2004: *Combined effects of tectonics and glacial isostatic adjustment on intra-plate deformation in central and northern Europe: applications to geodetic baseline analysis*. J. Geophys. Res., **109**, 1-22.

McClusky S., Balassanian S., Barka A., Demir C., Ergintav S., Georgiev I., Gurkan O., Hamburger M., Hurst K., Kahle H., Kastens K., Kekelidze G., King R., Kotzev V., Lenk O., Mahmoud S., Mishin A., Nadariya M., Ouzounis A., Paradissis D., Peter Y., Prilepin M., Reilinger R., Sanli I., Seeger H., Tealeb A., Toksoz M.N. and Veis G.; 2000: *Global Positioning System constraints on plate kinematics and dynamics in the eastern Mediterranean and Caucasus*. J. Geophys. Res., **105**, 5695-5719.

Nocquet J.M. and Calais E.; 2003: *Crustal velocity field of western Europe from permanent GPS array solutions, 1996-2001*. Geophys. J., Int., **154**, 72-88.

Nocquet J.M., Calais E., Altamini Z., Sillard P. and Boucher C.; 2001: *Intraplate deformation in western Europe deduced from an analysis of the International Terrestrial Reference Frame 1997 (ITRF97) velocity field.* J. Geophys. Res., **106**, 11239-11257.

Sabadini R., Di Donato G., Vermeersen L.L.A., Devoti R., Luceri V. and Bianco G.; 2002: *Ice mass loss in Antartica and stiff lower mantle viscosity inferred from the long wavelength time dependent gravity field*. Geophys. Res. Lett., **29**, 11/1-11/4.

Vermeersen L.L.A. and Sabadini R.; 1997: *A new class of stratified viscoelastic models by analytical techniques.* Geophys. J., Int., **129**, 531-570.

Wessel P. and Smith W.M.F.; 2001: *New improved version of Generic Mapping Tools released*. EOS, Trans. Am. Geophys. Union, **79**, 579.

Corresponding author: Anna Maria Marotta
Sezione Geofisica, Dipartimento di Scienze della Terra, Università di Milano
Via L. Cicognara 7, 20129 Milano, Italy
phone +39 02 50318470; fax +39 02 50318489
e-mail: anna.maria.marotta@unimi.it